Kennesaw State University
DigitalCommons@Kennesaw State University

Faculty Publications

8-1-2011

Top Quark Theoretical Cross Sections and pT and Rapiditiy Distributions

Nikolaos Kidonakis
Kennesaw State University, nkidonak@kennesaw.edu

Follow this and additional works at: https://digitalcommons.kennesaw.edu/facpubs

 Part of the Physics Commons

Recommended Citation
Kidonakis, Nikolaos, "Top Quark Theoretical Cross Sections and pT and Rapiditiy Distributions" (2011). *Faculty Publications*. 3866.
https://digitalcommons.kennesaw.edu/facpubs/3866

This Article is brought to you for free and open access by DigitalCommons@Kennesaw State University. It has been accepted for inclusion in Faculty Publications by an authorized administrator of DigitalCommons@Kennesaw State University. For more information, please contact digitalcommons@kennesaw.edu.

Top Quark Theoretical Cross Sections and p_T and Rapidity Distributions

Nikolaos Kidonakis
Kennesaw State University, Physics #1202, Kennesaw, GA 30144, USA

arXiv:1109.3231v1 [hep-ph] 15 Sep 2011

I present theoretical results for the top quark pair total cross section, and for the top quark transverse momentum and rapidity distributions at Tevatron and LHC energies. I also present results for single top quark production in the t- and s-channels and also via associated production with a W boson. The calculations include approximate NNLO corrections that are derived from NNLL soft-gluon resummation.

1. Introduction

The top quark is a very important part of the collider programs at the Tevatron and the LHC. Top quarks have been produced via top-antitop pair production and also via single top production at both colliders. The partonic processes at LO for top-antitop pair production are $q\bar{q} \to t\bar{t}$, dominant at the Tevatron, and $gg \to t\bar{t}$, dominant at the LHC. The leading-order (LO) diagrams are shown in Fig. 1.

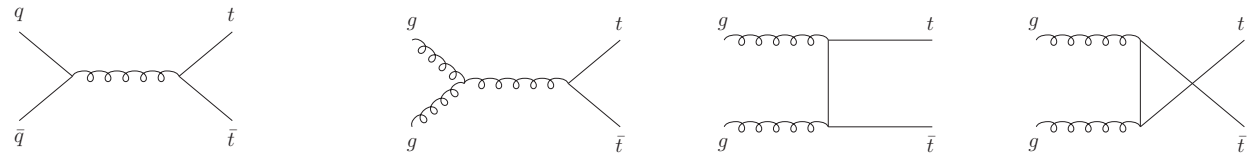

Figure 1: LO $q\bar{q} \to t\bar{t}$ and $gg \to t\bar{t}$ diagrams.

Single top quark production can proceed via the t-channel processes, the s-channel processes, and via associated production of a top quark with a W boson. The LO diagrams for these proceses are shown in Fig. 2.

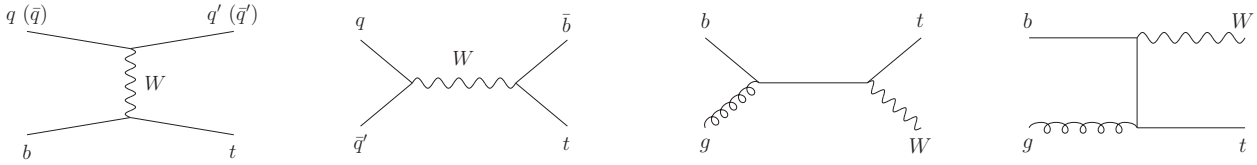

Figure 2: LO t-channel, s-channel, and tW diagrams.

The t-channel processes, $qb \to q't$ and $\bar{q}b \to \bar{q}'t$, are dominant at both the Tevatron and the LHC. The s-channel processes, $q\bar{q}' \to \bar{b}t$, are small at the Tevatron and LHC. The associated production of a top quark with a W boson, $bg \to tW^-$, has a very small cross section at the Tevatron, but is significant at the LHC. A related process to tW production is the associated production of a top quark with a charged Higgs boson in the Minimal Supersymmetric Standard Model, $bg \to tH^-$.

In Sec. 2 we discuss higher-order corrections for both $t\bar{t}$ and single-top production and identify soft-gluon corrections which are important near partonic threshold and contribute the dominant higher-order corrections in the hadronic cross section. In Sec. 3 we give results for the total top-antitop pair cross section. In Sec. 4 we show results for the top quark transverse momentum, p_T, distribution. In Sec. 5 we give results for the top quark rapidity, Y, distribution and the top quark forward-backward asymmetry. In Sec. 6 we present results for single top quark production via the t channel, in Sec. 7 via the s channel, and in Sec. 8 via associated production with a W. We conclude in Sec. 9 with a summary.

2. Higher-order corrections

QCD corrections are significant for top pair and single top quark production and are known fully at next-to-leading order (NLO). Soft-gluon corrections from emission of soft (low-energy) gluons are an important contributor to the QCD corrections. These soft-gluon corrections are dominant near threshold and they are of the form $[\ln^k(s_4/m^2)/s_4]_+$ with $k \leq 2n-1$ and s_4 the kinematical distance from threshold.

We can resum these soft corrections via factorization and renormalization-group evolution. At next-to-leading-logarithm (NLL) accuracy this requires one-loop calculations in the eikonal approximation. Complete results now exist at next-to-next-to-leading-logarithm (NNLL) accuracy, using the two-loop soft anomalous dimension matrices for the corresponding partonic subprocesses.

An approximate next-to-next-to-leading-order (NNLO) cross section is derived from the expansion of the resummed cross section [1, 2]. The calculation is at the differential cross section level using single-particle-inclusive (1PI) kinematics. We note that 1PI kinematics refer to partonic threshold, not just absolute threshold.

The threshold approximation works very well not only for Tevatron but also for LHC energies because partonic threshold is still important at the LHC: there is only a 1% difference between first-order approximate and exact corrections which translates into less than 1% difference between NLO approximate and exact cross sections.

For our best prediction for the total cross section and differential distributions we add the NNLO approximate corrections from NNLL resummation to the exact NLO results.

3. $t\bar{t}$ cross section

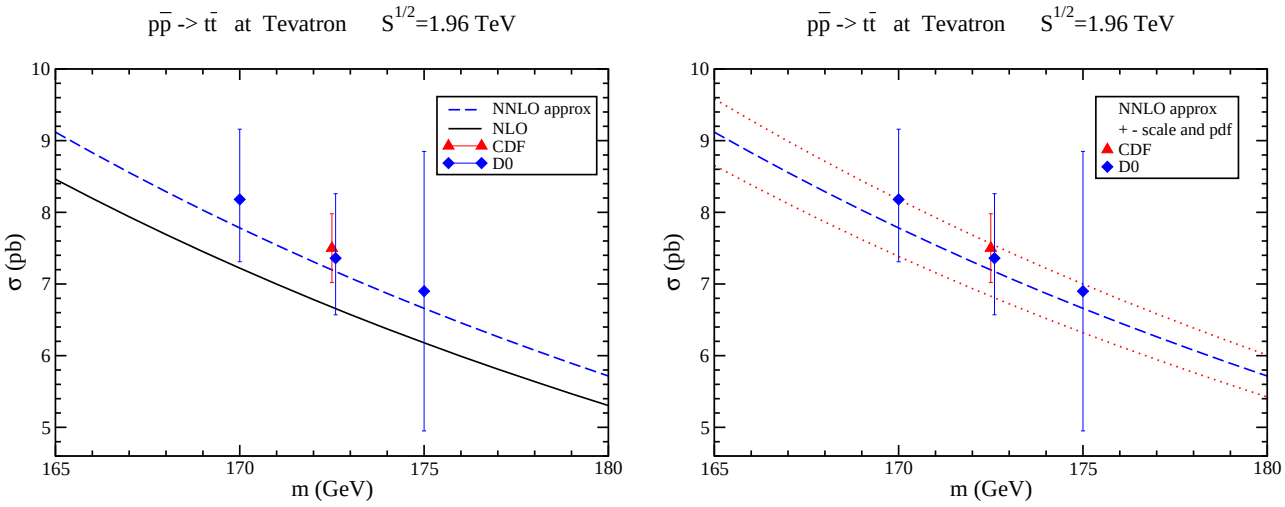

Figure 3: Cross section for $t\bar{t}$ production at the Tevatron.

We begin with the total top-antitop pair cross section. In Fig. 3 we show results for the exact NLO and the approximate NNLO cross section [1] at Tevatron energy and compare with recent results from the CDF [3] and D0 [4] Collaborations. The left plot shows that the NNLO approximate cross section describes the data better than NLO, while the plot on the right shows the approximate NNLO result together with the theoretical uncertainty, which is derived by varying the scale by a factor of two around the central value $\mu = m$ and adding this uncertainty in quadrature with the uncertainty from the MSTW2008 NNLO parton distribution functions (pdf) [5] at 90% C.L.

The $t\bar{t}$ cross section at the Tevatron for a top quark mass of 173 GeV is

$$\sigma_{t\bar{t}}^{\rm NNLOapprox}(m_t = 173\,{\rm GeV},\, 1.96\,{\rm TeV}) \;=\; 7.08^{+0.00+0.36}_{-0.24-0.27}\ {\rm pb}$$

where the first uncertainty is from scale variation and the second is from the pdf. The NNLO approximate corrections enhance the cross section by 7.8% over the NLO result (with the same pdf).

In Fig. 4 we show the scale dependence of the $t\bar{t}$ cross section at the Tevatron. The plot shows that the LO result displays a large dependence on the scale. The NLO cross section has a much milder dependence and the NNLO approximate result significantly reduces the dependence even further.

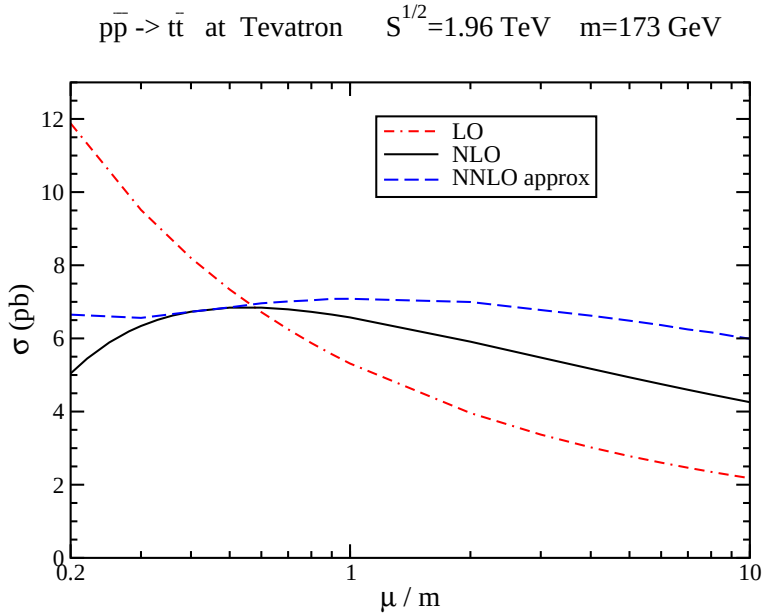

Figure 4: Scale dependence of the $t\bar{t}$ cross section at the Tevatron.

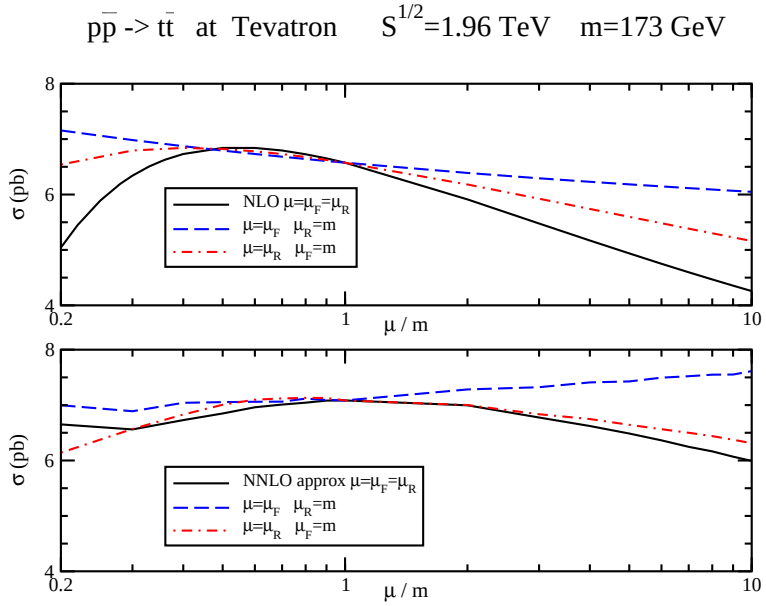

Figure 5: NLO and NNLO μ_F and μ_R dependence of the $t\bar{t}$ cross section at the Tevatron.

Figure 5 shows the separate dependence of the NLO and approximate NNLO cross sections on independent variations of the factorization scale μ_F and the renormalization scale μ_R. We observe a reduction at NNLO in the independent scale variations as well.

In Fig. 6 we show the $t\bar{t}$ cross section at the LHC at 7 TeV energy and compare with recent results from the ATLAS [6] and CMS [7] Collaborations. The left plot shows that the NNLO approximate cross section is in better agreement with the data than the NLO result. The plot on the right shows the central NNLO approximate cross section as before together with the uncertainty from scale variation and pdf errors.

The $t\bar{t}$ cross section for a top quark mass of 173 GeV at the LHC with 7 TeV energy is

$$\sigma_{t\bar{t}}^{\rm NNLOapprox}(m_t = 173\,{\rm GeV},\, 7\,{\rm TeV}) \;=\; 163^{+7+9}_{-5-9}\ {\rm pb}$$

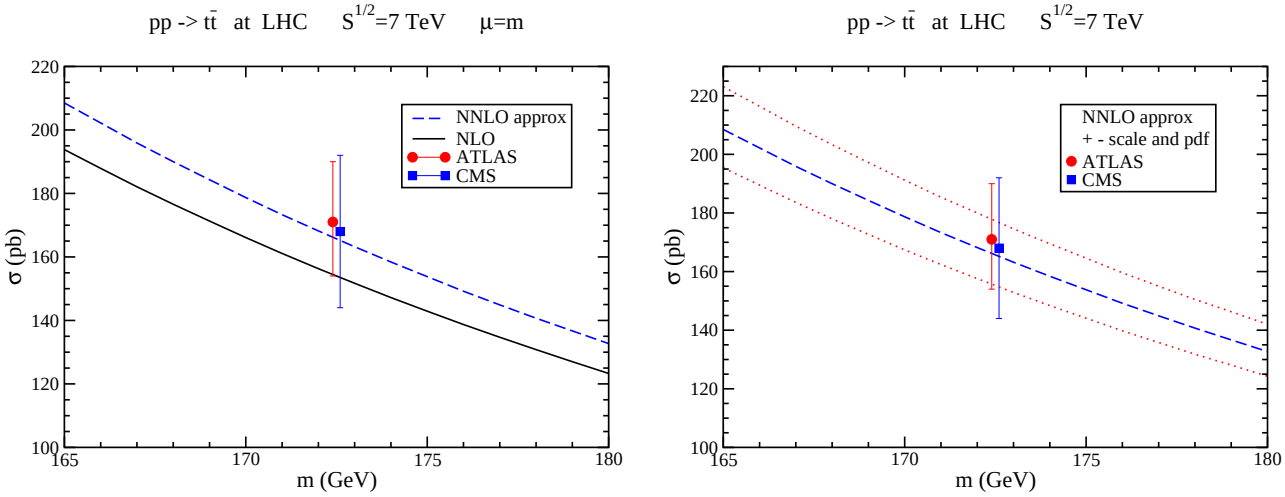

Figure 6: Cross section for $t\bar{t}$ production at the LHC.

while the corresponding result at 14 TeV energy is

$$\sigma_{t\bar{t}}^{\rm NNLOapprox}(m_t = 173\,{\rm GeV}, 14\,{\rm TeV}) \;=\; 920^{+50+33}_{-39-35}\;{\rm pb}\,.$$

The NNLO approximate corrections contribute an enhancement over NLO of 7.6% at 7 TeV and 8.0% at 14 TeV.

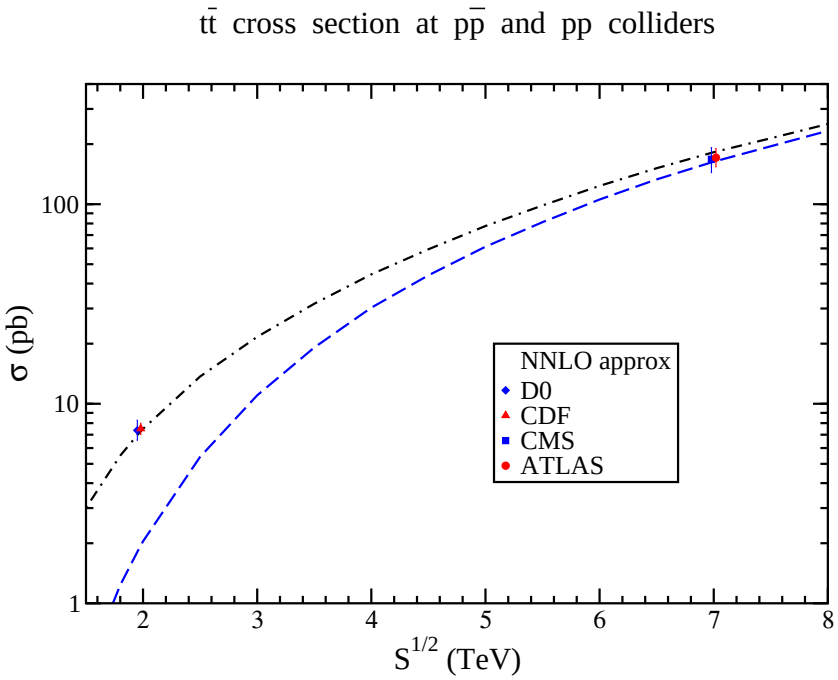

Figure 7: Cross section for $t\bar{t}$ production at $p\bar{p}$ and pp colliders.

Figure 7 plots the $t\bar{t}$ theoretical cross sections versus collider energy for $p\bar{p}$ and pp collisions together with experimental measurements of the cross section. The Tevatron and LHC data are in very good agreement with theory.

4. Top quark transverse momentum distributions

The top quark transverse momentum distribution, $d\sigma/dp_T$, at the Tevatron and at the LHC at 7 TeV is plotted in Fig. 8. NLO and approximate NNLO results [1] are displayed for the central scale value $\mu = m$ as well as for $\mu = m/2$ and $2m$.

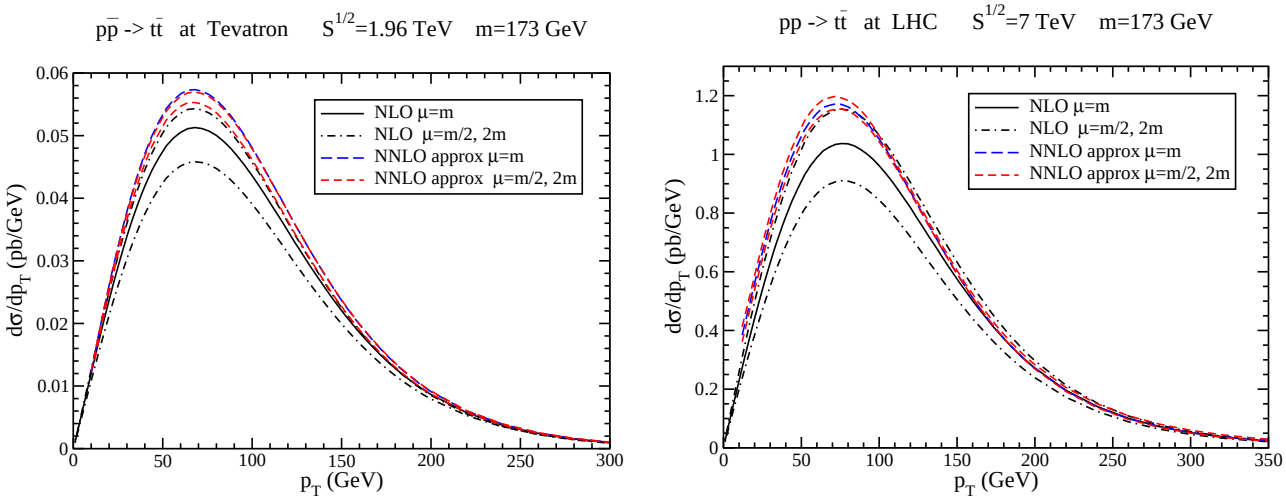

Figure 8: Top quark p_T distribution at the Tevatron and the LHC.

The NNLO soft-gluon corrections enhance the p_T distribution but they do not significantly change the shape in the p_T range shown. The scale dependence is reduced relative to NLO, in line with the reduction that was observed for the total cross section.

5. Top quark rapidity distributions and forward-backward asymmetry

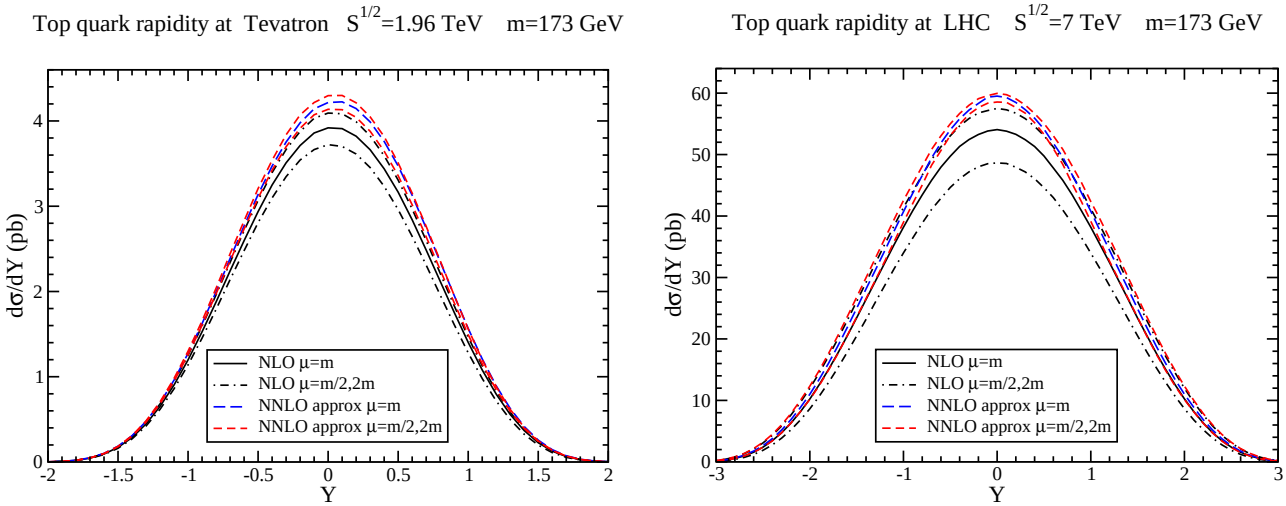

Figure 9: Top quark rapidity distribution at the Tevatron and the LHC.

The top quark rapidity distribution, $d\sigma/dY$, at the Tevatron and at the LHC at 7 TeV is plotted in Fig. 9. Again, NLO and approximate NNLO results [8] are displayed for the central scale value $\mu = m$ as well as for $\mu = m/2$ and $2m$. The NNLO soft-gluon corrections enhance the rapidity distribution and reduce the scale dependence relative to NLO but they do not significantly change the shape in the rapidity range shown.

The rapidity distribution enters into the definition of the forward-backward asymmetry,

$$A_{\rm FB} = \frac{\sigma(Y>0) - \sigma(Y<0)}{\sigma(Y>0) + \sigma(Y<0)}\,.$$

The gg channel is symmetric at all orders. The $q\bar{q}$ channel on the other hand is asymmetric starting at NLO. The asymmetry is significant at the Tevatron. The theoretical result for the top quark asymmetry at the Tevatron at approximate NNLO is $A_{\rm FB} = 0.052^{+0.000}_{-0.006}$ where the uncertainty indicated is from scale variation. The theoretical value is much smaller than current experimental values.

6. Single top quark production - t channel

The t-channel production of a single top quark proceeds via the exchange of a spacelike W boson. The process is dominant among single top channels at both Tevatron and LHC energies.

For a top quark mass of 173 GeV the approximate NNLO t-channel single top cross sections [9] are

$$\begin{aligned}
\sigma^{\rm NNLOapprox,\,top}_{t-{\rm channel}}(m_t = 173\,{\rm GeV},\,1.96\,{\rm TeV}) &= 1.04^{+0.00}_{-0.02} \pm 0.06\ {\rm pb} \\
\sigma^{\rm NNLOapprox,\,top}_{t-{\rm channel}}(m_t = 173\,{\rm GeV},\,7\,{\rm TeV}) &= 41.7^{+1.6}_{-0.2} \pm 0.8\ {\rm pb} \\
\sigma^{\rm NNLOapprox,\,top}_{t-{\rm channel}}(m_t = 173\,{\rm GeV},\,14\,{\rm TeV}) &= 151^{+4}_{-1} \pm 3\ {\rm pb}\,.
\end{aligned}$$

For t-channel single antitop production the cross section at the Tevatron is the same as for top. However, the single antitop production cross section at the LHC in the t channel is different:

$$\begin{aligned}
\sigma^{\rm NNLOapprox,\,antitop}_{t-{\rm channel}}(m_t = 173\,{\rm GeV},\,7\,{\rm TeV}) &= 22.5 \pm 0.5^{+0.7}_{-0.9}\ {\rm pb} \\
\sigma^{\rm NNLOapprox,\,antitop}_{t-{\rm channel}}(m_t = 173\,{\rm GeV},\,14\,{\rm TeV}) &= 92^{+2+2}_{-1-3}\ {\rm pb}\,.
\end{aligned}$$

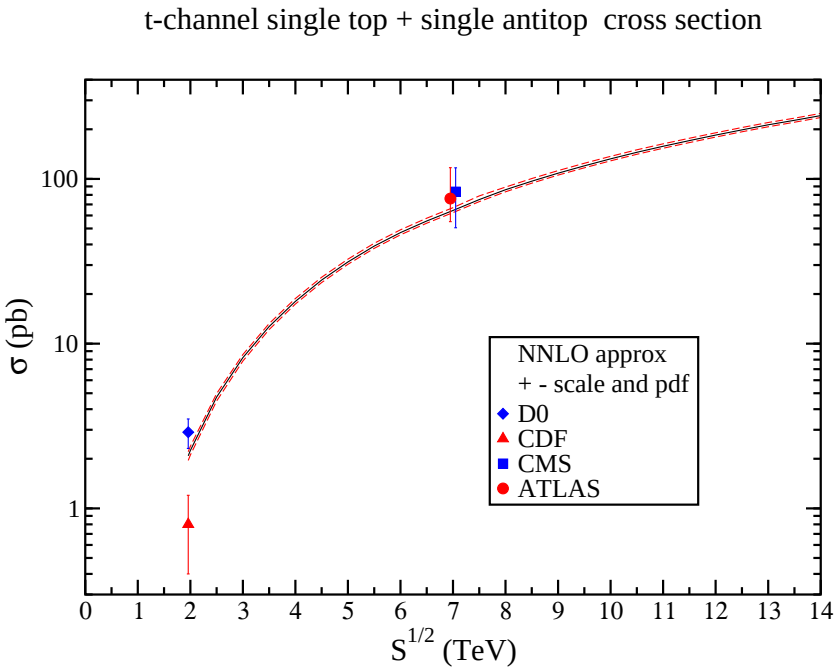

Figure 10: t-channel cross section at hadron colliders.

The t-channel combined cross section (single top + single antitop) is plotted versus energy in Fig. 10 together with recent measurements at the Tevatron [10, 11] and the LHC [12, 13]. Again the Tevatron and LHC results are consistent with theory.

7. Single top quark production - s channel

The s-channel production of a single top quark proceeds via the exchange of a timelike W boson. This process has the smallest cross section among single top channels at LHC energies.

For a top quark mass of 173 GeV the approximate NNLO s-channel single top cross sections [14] are

$$\begin{aligned}
\sigma_{s-\mathrm{channel}}^{\mathrm{NNLOapprox,\,top}}(m_t = 173\,\mathrm{GeV},\, 1.96\,\mathrm{TeV}) &= 0.523^{+0.001+0.030}_{-0.005-0.028}\ \mathrm{pb} \\
\sigma_{s-\mathrm{channel}}^{\mathrm{NNLOapprox,\,top}}(m_t = 173\,\mathrm{GeV},\, 7\,\mathrm{TeV}) &= 3.17 \pm 0.06^{+0.13}_{-0.10}\ \mathrm{pb} \\
\sigma_{s-\mathrm{channel}}^{\mathrm{NNLOapprox,\,top}}(m_t = 173\,\mathrm{GeV}, 14\,\mathrm{TeV}) &= 7.93 \pm 0.14^{+0.31}_{-0.28}\ \mathrm{pb}\,.
\end{aligned}$$

The NNLO approximate corrections provide an enhancement over NLO (with the same pdf) of 15% at the Tevatron and 13% at the LHC, and thus they have a very significant impact.

The s-channel single antitop production cross section at the Tevatron is the same as for top. However, the s-channel single antitop production cross section at the LHC is different:

$$\begin{aligned}
\sigma_{s-\mathrm{channel}}^{\mathrm{NNLOapprox,\,antitop}}(m_t = 173\,\mathrm{GeV},\, 7\,\mathrm{TeV}) &= 1.42 \pm 0.01^{+0.06}_{-0.07}\ \mathrm{pb} \\
\sigma_{s-\mathrm{channel}}^{\mathrm{NNLOapprox,\,antitop}}(m_t = 173\,\mathrm{GeV}, 14\,\mathrm{TeV}) &= 3.99 \pm 0.05^{+0.14}_{-0.21}\ \mathrm{pb}\,.
\end{aligned}$$

8. Associated tW^- production

The associated production of a top quark with a W boson, $bg \to tW^-$, is negligible at the Tevatron but important at the LHC. For a top quark mass of 173 GeV the approximate NNLO cross section [15] is

$$\begin{aligned}
\sigma_{tW}^{\mathrm{NNLOapprox}}(m_t = 173\,\mathrm{GeV},\, 7\,\mathrm{TeV}) &= 7.8 \pm 0.2^{+0.5}_{-0.6}\ \mathrm{pb} \\
\sigma_{tW}^{\mathrm{NNLOapprox}}(m_t = 173\,\mathrm{GeV}, 14\,\mathrm{TeV}) &= 41.8 \pm 1.0^{+1.5}_{-2.4}\ \mathrm{pb}\,.
\end{aligned}$$

The NNLO approx corrections increase the NLO cross section by $\sim 8\%$. The cross section for $\bar{t}W^+$ production is identical to that for top.

A related process is the associated production of a top quark with a charged Higgs in the Minimal Supersymmetric Standard Model. In that case the NNLO approximate corrections increase the NLO cross section by ~ 15 to $\sim 20\%$. Another related process is W production at large p_T [2, 16].

9. Summary

We have discussed NNLL soft-gluon resummation for top quark pair and single top production. We have derived NNLO approximate cross sections from the expansion of the NNLL resummed cross section. Numerical results for the $t\bar{t}$ production cross section have been presented at both Tevatron and LHC energies. The NNLO approximate corrections reduce the scale dependence of the cross section.

The top quark p_T and rapidity distributions have also been presented and, again, the NNLO soft-gluon corrections enhance the cross section and reduce the scale dependence but they do not significantly affect the shape of the distributions. The theoretical top quark forward-backward asymmetry has also been calculated and is found to be significantly smaller than observed at the Tevatron.

The cross sections for t-channel and s-channel single top production as well as the associated production of a top quark with a W boson have also been presented at both Tevatron and LHC.

The NNLO approximate corrections for top pair and single top production are significant at both the Tevatron and LHC colliders and they reduce the theoretical uncertainty. The theoretical results are in good agreement with experimental measurements from CDF and D0 at the Tevatron, and from ATLAS and CMS at the LHC.

Acknowledgments

This work was supported by the National Science Foundation under Grant No. PHY 0855421.

References

1 N. Kidonakis, Phys. Rev. D **82**, 114030 (2010) [arXiv:1009.4935 [hep-ph]].
2 N. Kidonakis, in *DPF-2011*, arXiv:1109.1578 [hep-ph].
3 CDF Collaboration, Conf. Note 9913.
4 D0 Collaboration, Phys. Rev. D **80**, 071102(R) (2009) [arXiv:0903.5525 [hep-ex]]; Phys. Rev. D **82**, 032002 (2010) [arXiv:0911.4286 [hep-ex]]; arXiv:1105.5384v1 [hep-ex].
5 A.D. Martin, W.J. Stirling, R.S. Thorne, and G. Watt, Eur. Phys. J. C **63**, 189 (2009) [arXiv:0901.0002 [hep-ph]].
6 ATLAS Collaboration, ATLAS-CONF-2011-100.
7 CMS Collaboration, JHEP **07**, 049 (2011) [arXiv:1105.5661 [hep-ex]].
8 N. Kidonakis, Phys. Rev. D **84**, 011504 (2011) [arXiv:1105.5167 [hep-ph]].
9 N. Kidonakis, Phys. Rev. D **83**, 091503 (2011) [arXiv:1103.2792 [hep-ph]].
10 CDF Collaboration, Phys. Rev. D **82**, 112005 (2010) [arXiv:1004.1181 [hep-ex]].
11 D0 Collaboration, arXiv:1105.2788 [hep-ex].
12 ATLAS Collaboration, ATLAS-CONF-2011-088.
13 CMS Collaboration, arXiv:1106.3052 [hep-ex].
14 N. Kidonakis, Phys. Rev. D **81**, 054028 (2010) [arXiv:1001.5034 [hep-ph]].
15 N. Kidonakis, Phys. Rev. D **82**, 054018 (2010) [arXiv:1005.4451 [hep-ph]].
16 N. Kidonakis and A. Sabio Vera, JHEP **02**, 027 (2004) [hep-ph/0311266]; N. Kidonakis and R.J. Gonsalves, in *DPF-2011*, arXiv:1109.2817 [hep-ph].